ELSEVIER

Intermetallics 7 (1999) 479–489

Intermetallics

Micromechanisms of fracture in NiAl studied by in situ straining experiments in an HVEM

D. Baither [a,*], F. Ernst [a], T. Wagner [a], M. Rühle [a], M. Bartsch [b], U. Messerschmidt [b]

[a] *Max-Planck-Planck Institut für Metallforschung, Seestr. 92, D-70174 Stuttgart, Germany*
[b] *Max-Planck-Institut für Mikrostrukturphysik, Weinberg 2,D-06120 Halle/Saale, Germany*

Received 27 April 1998; revised 23 July 1998; accepted 16 September 1998

Abstract

The room temperature brittleness of NiAl constitutes a major problem for technical applications. In order to investigate the micromechanisms of fracture in NiAl, we have carried out in situ tensile straining experiments on stoichiometric NiAl single crystals in a high-voltage electron microscope. According to our observations, crack propagation always involves dislocation activity around the crack tip, even in the hard orientation at room temperature. The Burgers vectors and the typical arrangements of the dislocations, as well as the extension of the corresponding plastic zone vary with the loading direction and the orientation of the microcrack versus potential glide systems. We observe that local concentrations of slip leads to irregular deviation of the cleavage plane from the {1 1 0} facets one usually observes at the macroscopic level. The results of our experiments help to understand why the mode I fracture toughness of NiAl is significantly larger for ⟨1 0 0⟩ loading directions than for non-⟨1 0 0⟩ directions.

Keywords: Nickel aluminides; Based on NiAl; Fracture toughness; Defects: dislocation geometry and arrangement; Electron microscopy

1. Introduction

Stoichiometric NiAl is a promising material for applications at intermediate temperatures, especially owing to its good oxidation resistance [1,2]. At room temperature (RT), however, the material has a poor ductility. Hypotheses about the origin of the RT brittleness include inadequate slip systems, low dislocation mobility, inhomogeneous slip, and low fracture stress [3]. In NiAl single crystals, the deformation behaviour strongly depends on the loading direction. When loading along non-⟨1 0 0⟩ directions ('soft directions') NiAl exhibits some tensile ductility, while when loading along ⟨1 0 0⟩ directions the material is very brittle. At room temperature, single crystals typically fail by cleavage on {1 1 0} planes. However, cleavage along high-index planes was reported, too [4]. Until now it has not been clarified whether cracks propagate by atomistic cleavage at the tip alone, or require the emission of dislocations. The details of the plastic deformation near crack tips are not well known [5]. In order to advance the understanding of the underlying processes on the microscopic scale, we have carried out in situ fracture experiments in a high-voltage transmission electron microscope (HVEM). The present paper is restricted to room temperature experiments. In a subsequent paper we will report on in situ observations we have carried out at high temperature in order to promote the understanding of the brittle-to-ductile transition of NiAl.

2. Experimental

Nominally stoichiometric NiAl single crystals were grown by induction melting. The in situ experiments in the quantitative tensile double-tilting stage [6] of the HVEM require micro-tensile samples of 8 mm in length and about 2 mm in width. These samples were ground

* Corresponding author present address: Westfälische Wilhelms-Universität, Institut für Metallforschung, Wilhelm-Klemm-Str.10, D-48149 Münster, Germany. Tel.: +49 251 83 39016; fax: +49 251 38346; e-mail: baither@uni-muenster.de

0966-9795/99/$ - see front matter
PII: S0966-9795(98)00106-X

to a thickness of 0.1 mm, and subsequently thinned by a two-step electrolytic jet-polishing procedure [7]. In the first step of the latter, the sample is covered by an aperture with a small hole (I in Fig. 1), such that a depression forms only at the centre of the sample. Then, an aperture with a larger hole is used (II in Fig. 1) to thin the sample over its whole width and to reduce the central cross-section. By balancing the relative contribution of each polishing step one obtains electron-transparent regions extending over several tenths of millimetres. Such large electron-transparent regions constitute a prerequisite to follow the crack propagation during an in situ straining experiment. Moreover, the cross section of the sample is sufficiently reduced to enable deformation under the maximum force of about 15 N one can apply in the HVEM straining stage. We used the above procedure to make TEM samples with (1 1 0) and (1 0 0) surfaces. Samples with (1 1 0) foil surfaces were prepared for tensile directions of $[1\bar{1}0]$, $[1\bar{1}1]$, $[1\bar{1}4]$, and [0 0 1], while samples with (1 0 0) surfaces were prepared for tensile directions of [0 1 1], [0 1 2], [0 1 4], and [0 0 1]. In situ experiments were carried out in an HVEM (JEM 1000) at an accelerating voltage of 1000 kV. The samples were loaded in small increments. Crack and dislocation structures were recorded on photographic film under nearly constant load. While increasing the load, we recorded the propagation of crack tips and dislocations on video tape. Usually, we unloaded the sample before catastrophic fracture and subsequently investigated the details of the crack and dislocation structure formed under loading *post mortem* in a wide-angle goniometer.

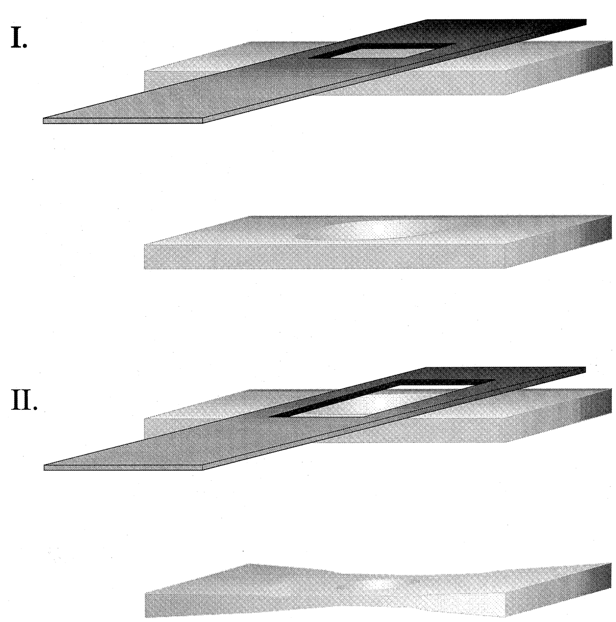

Fig. 1. Schematic drawing of the platinum masks and NiAl samples used in the two step electrolytic jet polishing.

3. Results

3.1. *Straining in 'soft' orientations*

3.1.1. $[1\bar{1}0]$ *tensile direction, (1 1 0) foil surfaces*

During tensile straining in $[1\bar{1}0]$ direction, crack propagation competes with localized plastic deformation near the crack tip. The micrographs in Fig. 2

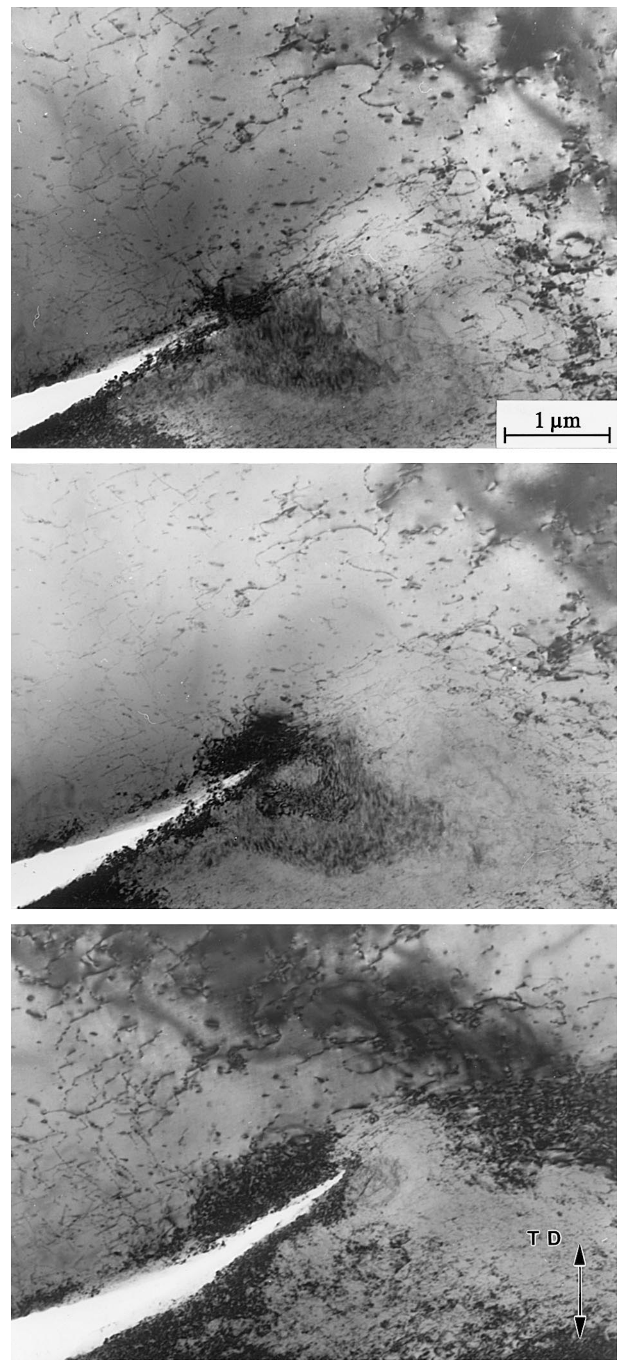

Fig. 2. Crack propagation and plastic zone during in situ straining in $[1\bar{1}0]$ tensile direction (TD). (1 1 0) Foil surfaces. The micrographs are taken in time intervals of about 5 s.

belong to a sample with a (1 1 0) surface. They were recorded at nearly the same position, in intervals of about 5 s. From Fig. 2(a) to (b) the density of dislocations ahead of the crack tip strongly increases, with the crack gradually propagating. After penetrating the plastic zone, as apparent in Fig. 2c, the crack propagates much faster into the less distorted region behind the plastic zone. This cycle recurred several times as long as we kept the external stress nearly constant. On the average, cleavage occurred approximately parallel to the (1 0 1) plane (inclined with respect to the surface). On the microscopic scale, however, we observe a strong influence of the local plastic deformation on the direction of the crack propagation. Fig. 3 shows different stages of crack growth. When the crack tip reaches the zone of high plastic deformation, the crack growth slows down and the crack opening increases (Fig. 3a). Then the crack smoothly deviates from its former direction, and forms a narrow cleavage (Fig. 3b). After passing the zone of maximum dislocation density, the crack returns to its former direction, i.e. a shift occurs from the original (1 0 1) cleavage plane onto a parallel (1 0 1) one (Fig. 2c).

Fig. 4 shows several very early stages of dislocation emission at a crack tip. In this initial stage, dislocations

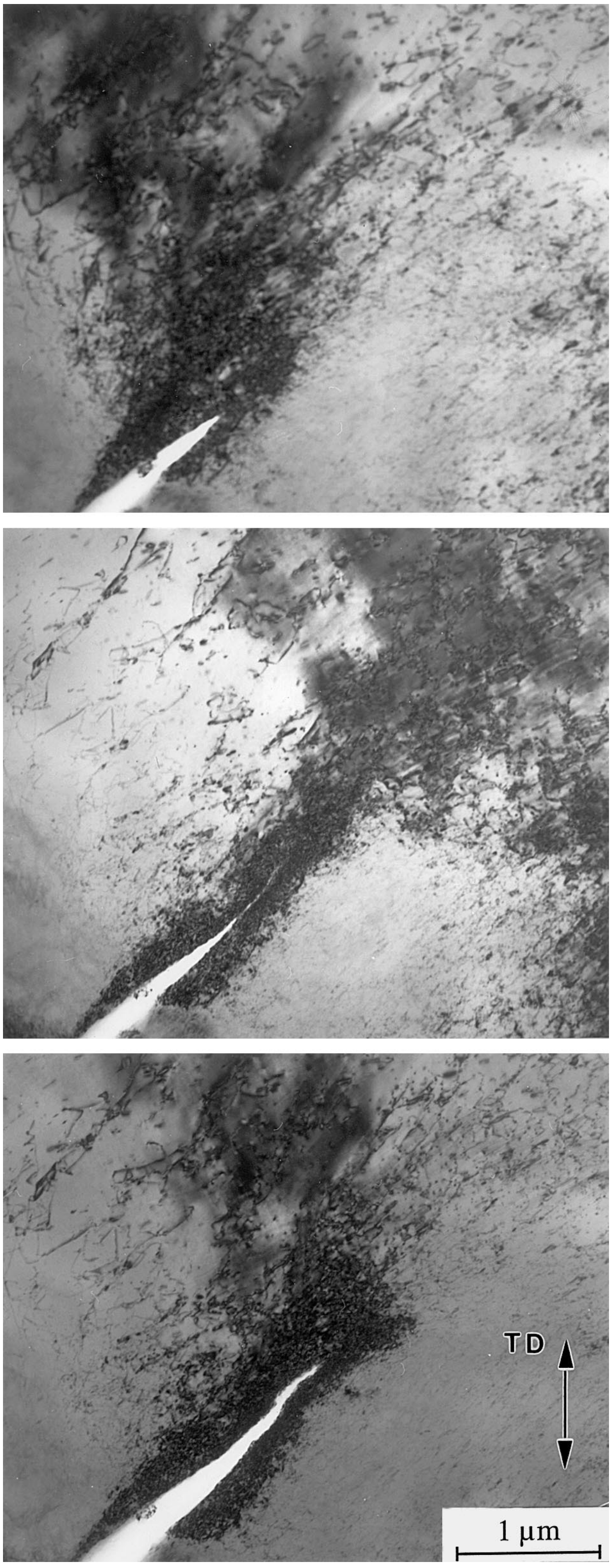

Fig. 3. Change of the crack direction in the sample of Fig. 2. The micrographs are taken in time intervals of about 5 s.

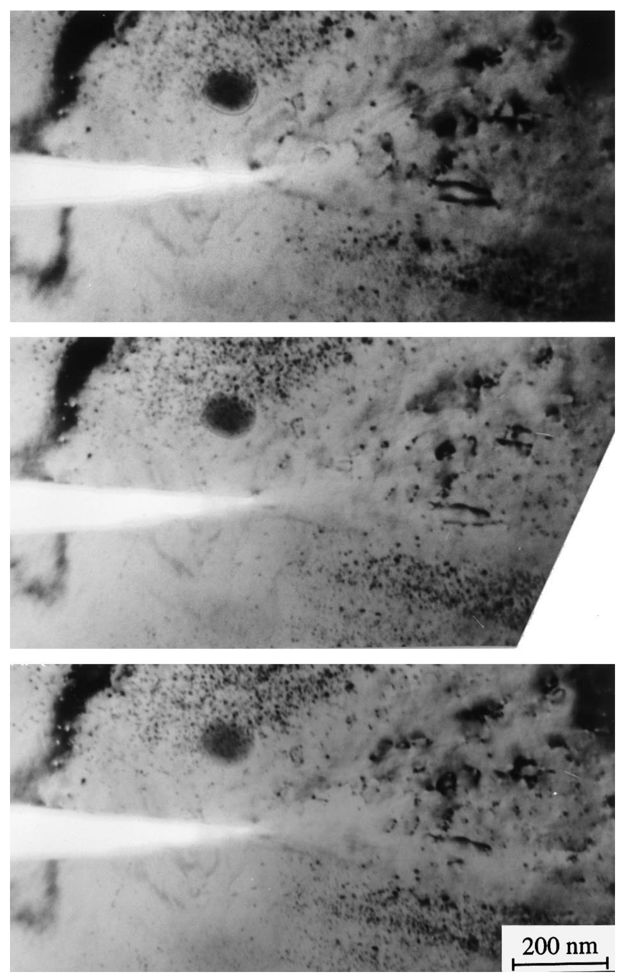

Fig. 4. Dislocation emission at the crack tip. [1 $\bar{1}$ 0] tensile direction and (1 1 0) foil surfaces.

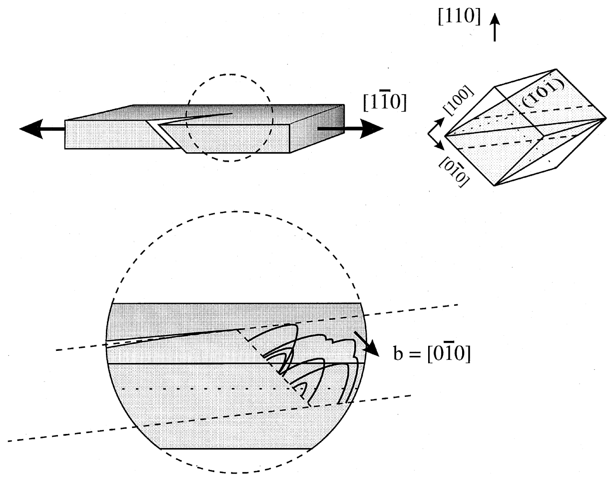

Fig. 5. Schematic drawing of the specimen, crack and slip geometry at straining in [1 $\bar{1}$ 0] direction.

with [1 0 0] and [0 1 0] Burgers vectors nucleate and glide on the four {1 1 0} planes inclined to the surface. We often observe cross-slip onto orthogonal {1 1 0} slip planes. As a consequence, most of the dislocations nucleating at the crack tip move into a fan-shaped region, which is bounded by the ⟨1 1 1⟩ intersection lines of the inclined {1 1 0} planes with the surface. At further straining and increasing foil thickness, dislocations on one {1 1 0} plane dominate, which is identical with the cleavage plane. Sometimes, however, changes of the slip system occur within the four possible ones mentioned above, as well as changes of the crack flanks or direction.

In front of the crack tip dislocation half loops move several ten micrometers into the crystal. The slip plane and the characteristic shape of these dislocation half-loops are drawn schematically in Fig. 5. Video frames

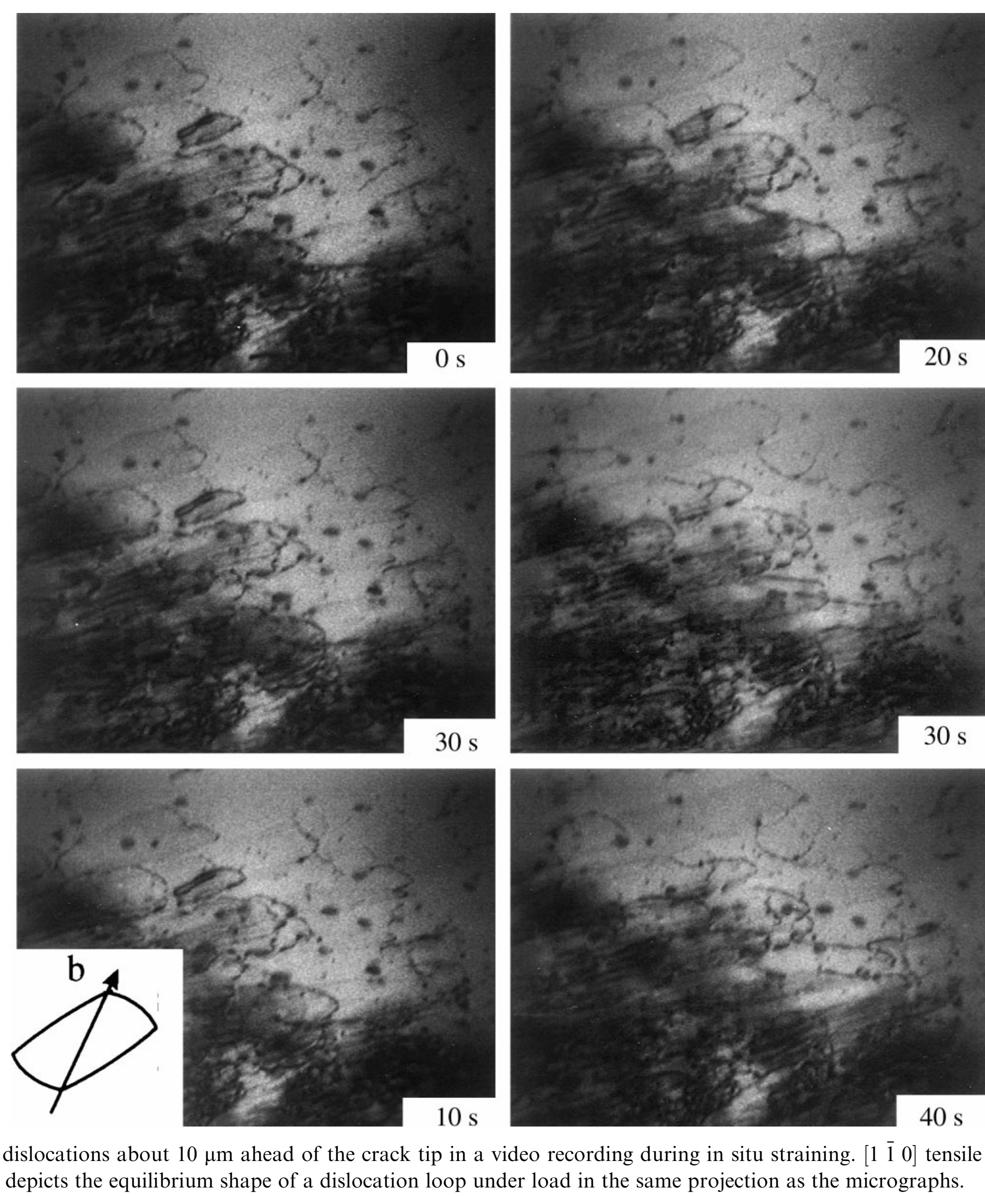

Fig. 6. Motion of dislocations about 10 μm ahead of the crack tip in a video recording during in situ straining. [1 $\bar{1}$ 0] tensile direction and (1 1 0) surfaces. The inset depicts the equilibrium shape of a dislocation loop under load in the same projection as the micrographs.

recorded at intervals of several seconds are reproduced in Fig. 6 and clarify the actual shape. Moreover, the frames reflect a viscous motion of the dislocations. The angular shape of the dislocation half loops follows from the anisotropy of the dislocation line tension [8]. Considering the elastic anisotropy of NiAl single crystals, the equilibrium shape of dislocation loops was calculated, and a drawing based on these calculations is inserted in Fig. 6. The result fits the shape of experimentally observed dislocation, including the strong bending, which originates from instability of segments with screw character.

During dislocation motion, dislocation loops were often dragged by the pinning of segments. In the course of further straining these loops act as dislocation sources. Examples are presented in the sequence of micrographs in Fig. 7. On the other hand, the dislocation loops may inhibit further dislocation motion. As obstacles, they cause the dislocations to pile-up, and later on to cross-slip onto the (1 0 0) plane in an avalanche-like way. An indication of this process is visible in Fig. 1(a) and (b), right below the crack tip. Other variants of $\langle 1 0 0\rangle\{1 1 0\}$ slip systems were often activated in such cases, too.

3.1.2. $[1\bar{1}1]$ tensile direction, (1 1 0) foil surfaces

If the straining direction is changed from $[1\bar{1}0]$ to $[1\bar{1}1]$, the crack runs irregularly, and the plastic deformation extends over a much wider region than that of the former case. Fig. 8 shows an overview of the microstructure. Compared to straining in $[1\bar{1}0]$ direction, additional slip systems with their [0 0 1] Burgers vectors parallel to the surface were activated by the external stress.

Particularly, many elongated dislocations appear on the $(1\bar{1}0)$ glide plane which is oriented edge-on with respect to the foil surfaces. Examples of such dislocations are shown in the micrographs of Fig. 9. Their screw segments lie nearly parallel to the surface over distances of several micrometers. All of them are heavily jogged and can easily cross-slip, probably on the (1 1 0)

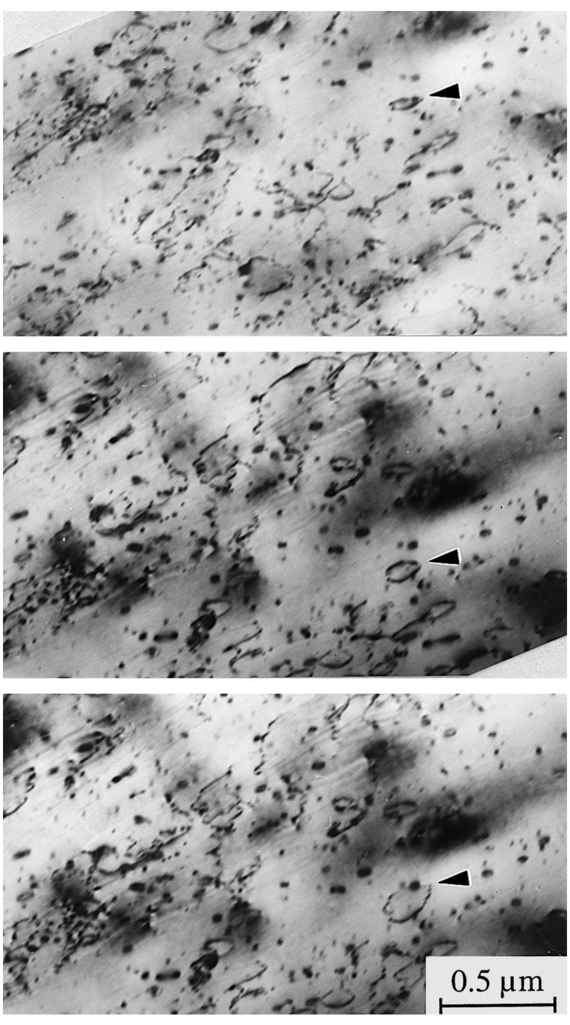

Fig. 7. Expanding dislocation loops ahead of the crack tip during in situ straining in $[1\bar{1}0]$ direction. (1 1 0) foil surfaces.

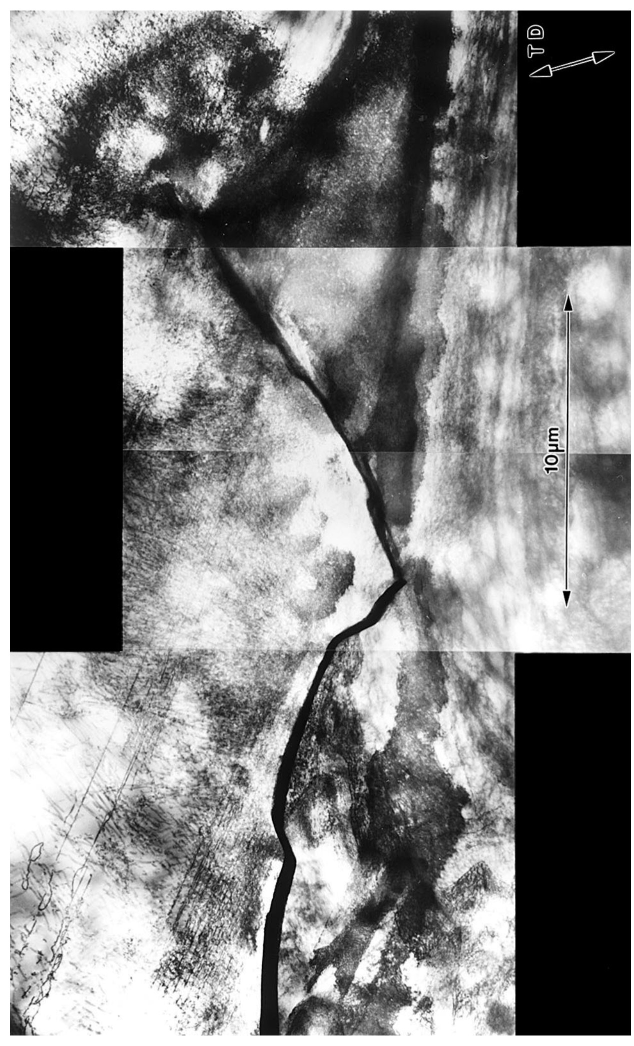

Fig. 8. Crack and dislocation structure after in situ straining in $[1\bar{1}1]$ direction. (1 1 0) foil surfaces.

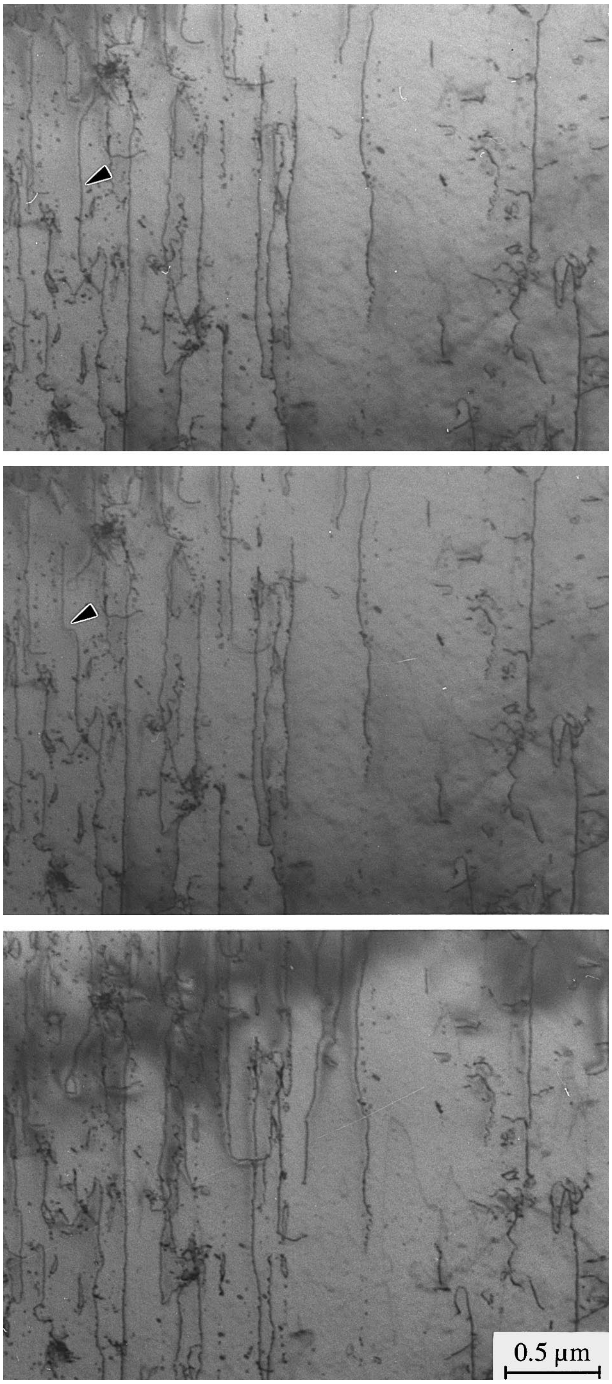

Fig. 9. Screw dislocations caused by crack growth during straining in $[1\,\bar{1}\,1]$ direction. The micrographs are taken in time intervals of about 5 s. (1 1 0) foil surfaces. The arrows mark a cross-slip event.

Fig. 10. Overview of the crack and the dislocation structure after in situ straining in [0 0 1] direction. (1 0 0) foil surfaces.

plane parallel to the surface. If a screw dislocation escapes through the foil surface, it leaves behind much debris – numerous small dislocation loops with mean diameters of about 10 nm.

The dislocations of the different slip systems interact with each other and mutually inhibit their motion. Thus, a more complex dislocation structure develops, which hinders further crack propagation and causes the crack to change its direction frequently. Hence, the crack either propagates along the {1 1 0} planes of different inclination with respect to the foil surface or jumps to the (1 1 0) plane oriented edge-on.

3.2. Straining in the 'hard' directions

3.2.1. [0 0 1] tensile direction, (1 0 0) foil surfaces

In the following, we mainly discuss straining along the [0 0 1] direction for samples with (1 0 0) surfaces.

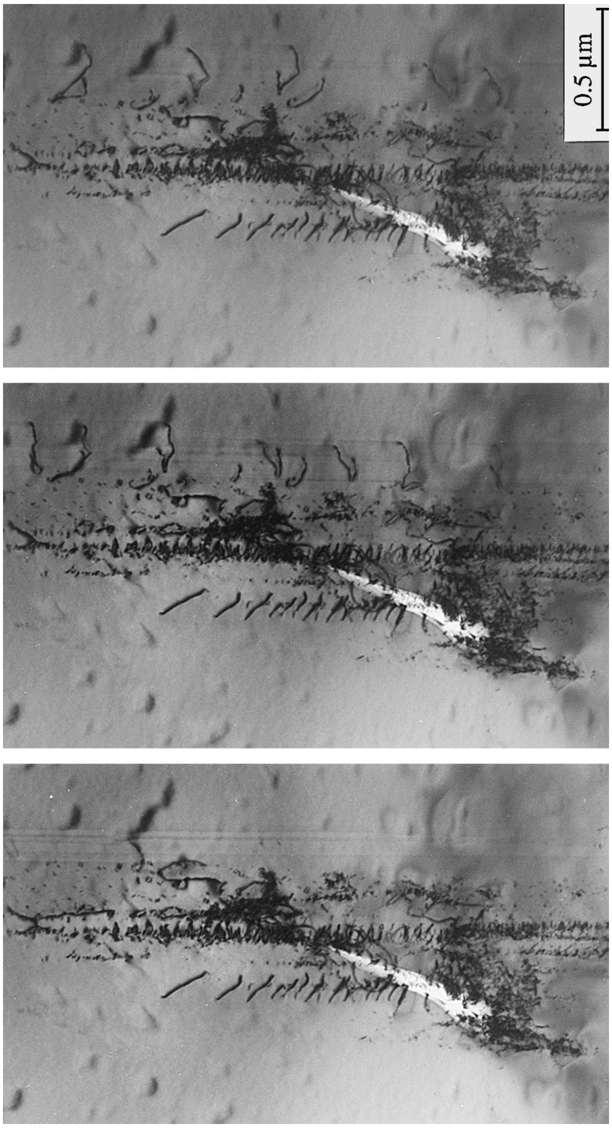

Fig. 11. Early stages of crack propagation and the formation of slip bands during straining in [0 0 1] direction. (1 0 0) foil surfaces.

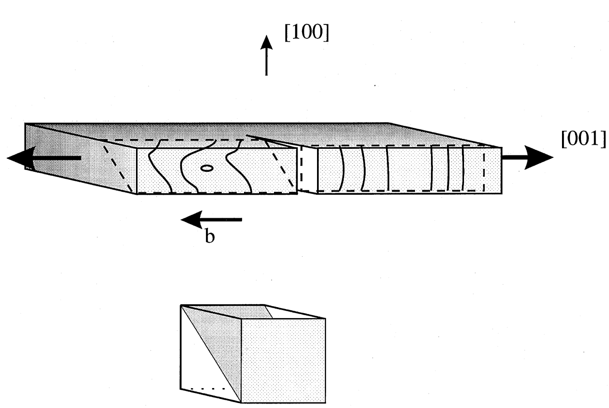

Fig. 12. Schematic drawing of the specimen, crack and slip geometry at straining in [0 0 1] direction.

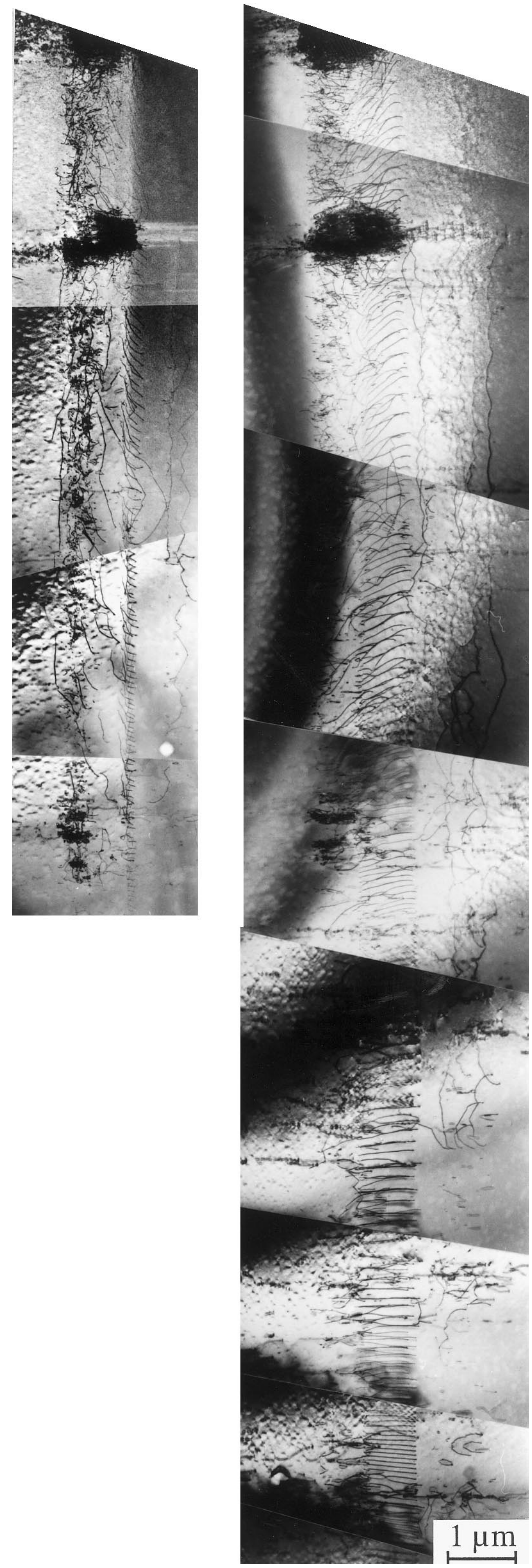

Fig. 13. Dislocation slip bands created at the crack tip during straining in [0 0 1] direction as shown in Fig. 10 imaged at different zone axes: (a) [1 0 0]; (b) near [1 1 0].

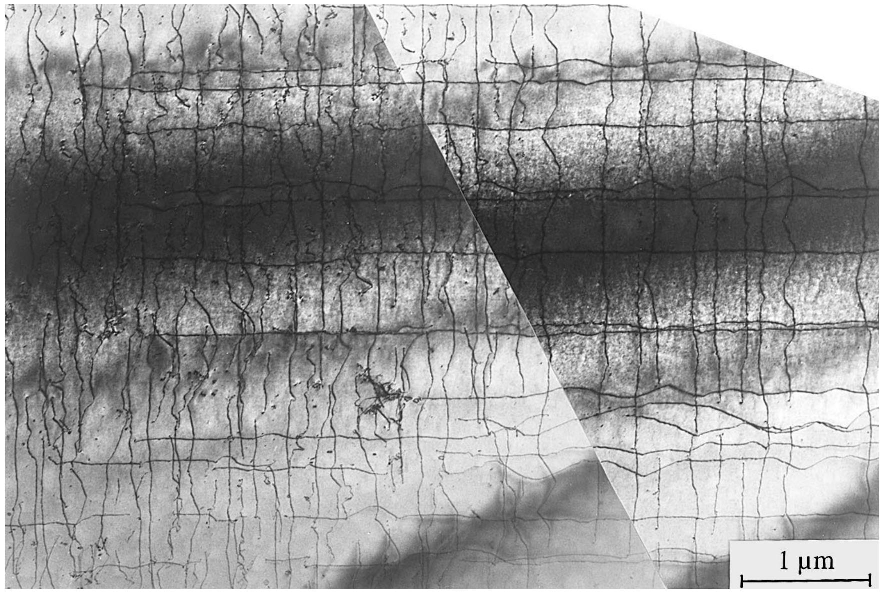

Fig. 14. Dislocation networks parallel to the surface caused by interacting slip bands: [0 0 1] tensile direction and (1 0 0) foil surfaces.

Samples with (1 1 0) surfaces behave similarly if loaded along [0 0 1]. Fig. 10 shows a typical example of crack propagation and the defects it creates. Characteristic features comprise an irregular path of the crack, elongated dislocation bands, and particular of dislocations in the immediate vicinity of the crack.

In contrast to straining in 'soft' directions, straining along a [0 0 1] direction causes the crack to propagate instantaneously over longer distances. Then the crack always stops in front of a dislocation band. The nucleation of such slip bands has never directly been observed; even the time resolution of 0.04 s enabled by the video system was not sufficient. The bands appear at the very moment the crack jumps. Unique cleavage planes can hardly be identified. In most cases, the crack flanks are bent or have a fractal appearance down to the sub-micrometer range. Early stages of the crack growth are shown in Fig. 11, however, some dislocation bands exist already.

The dislocation bands extend in $\langle 1\,0\,0\rangle$ directions, usually nearly orthogonal to the crack; this means that dislocation bands dominate which are parallel to the tensile direction. Sometimes, however, bands occur in the orthogonal direction, i.e. parallel to the crack, probably related to a local change in the direction of crack propagation. All dislocations in the bands have Burgers vectors of the type $\langle 1\,0\,0\rangle$ parallel to the extension of the band. As glide planes, different variants were observed with a common zone axis parallel to the direction of the band. Examples are schematically drawn in Fig. 12. The micrograph of Fig. 13a, recorded near the [1 0 0] pole, shows two parallel, closely neighbored bands, formed by dislocations on different slip planes. In the slip band on the right-hand side of Fig. 13a, the dislocations are oriented nearly end-on. After the specimen was tilted by about 45° around an axis parallel to the dislocation slip band, the dislocations were well imaged, as shown in Fig. 13b. The comparison of the two micrographs reveals that these dislocations are arranged on (0 1 0) slip planes. The extremely small width of the slip band and the nearly equidistant arrangement of the dislocations indicate that almost all dislocations lie on the same crystallographic plane. In contrast to that, the slip band on the left-hand side is less regular. The (1 1 0) plane dominates, but many dislocation segments randomly deviate from this plane. While in the (0 1 0) slip band only edge dislocation segments remained in the foil and long trailing screw segments were never observed during dislocation motion, the other band features some segments with mixed or screw character parallel to the surface. Consequently, cross-slip occurs, and generates dislocation loops. Differences between the two types of slip bands also exist with respect to the dislocation mobility. The edge dislocations in the (0 1 0) slip band move much faster over very long distances. We observed corresponding dislocations 100 μm away from the crack tip, observations further away were only limited by the increased foil thickness.

A particular dislocation arrangement arises when orthogonal slip bands are intersecting each other. In this case, the dislocations of both bands mutually inhibit their motion. As a result, screw dislocations form parallel to the surface also in the slip bands on the (0 1 0) plane, since these dislocations interact with the corresponding dislocations from the orthogonal band and cannot escape to the surface. A rather stable dislocation network forms nearly parallel to the surface, as shown

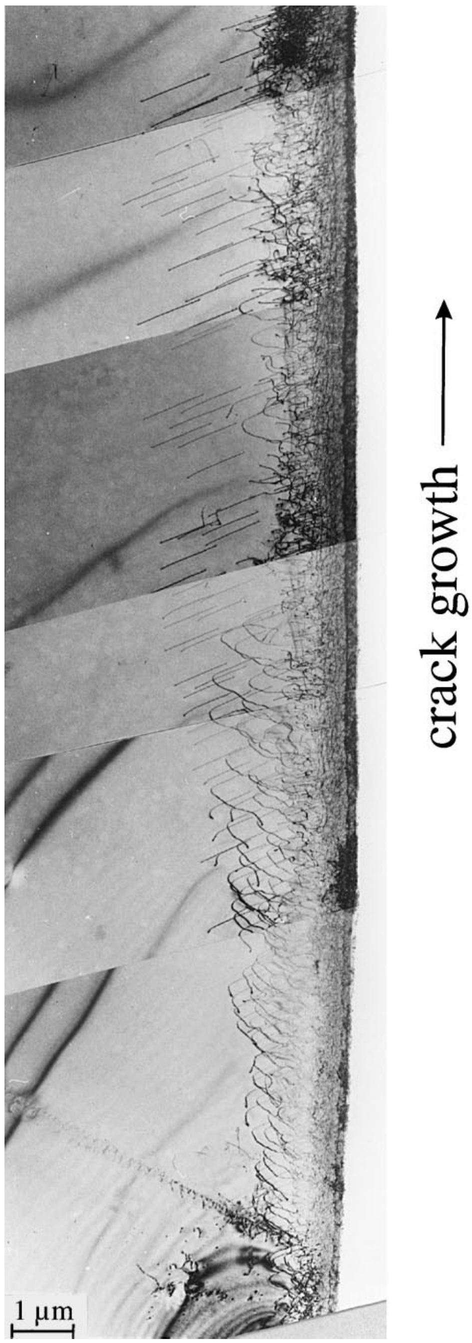

Fig. 15. Dislocations at the crack face with a [1 $\bar{1}$ 1] Burgers vector. [0 0 1] tensile direction and (1 0 0) foil surfaces.

in Fig. 14. The dislocation segments are pinned at the nodes and bow out towards the surface. In this configuration, screw dislocation segments are unable to cross-slip such that loops are not created within this structure.

Finally, we describe the dislocations very near to the crack faces in more detail. These dislocations were instantaneously created while the crack jumped to the next dislocation band, as described above. In samples with (1 0 0) surfaces the creation and motion of dislocations could not be observed or resolved in subsequent video frames, respectively. Fig. 15 shows an example of such dislocations, which were always found at the crack faces, without any exception. An outstanding feature of these dislocations is that most of them are ideally straight and have a line direction of ⟨1 1 1⟩. Unlike all other dislocations mentioned above they have ⟨1 1 1⟩ Burgers vectors, even though the straight segments have pure screw character. In addition to the straight, needle-like screw dislocations, half loops and elongated dislocations parallel to the crack faces are recognizable, all of them with the same Burgers vector. The shape and the (1 0 $\bar{1}$) glide plane of the dislocation half loops are schematically drawn in Fig. 16. Besides the glide plane indicated in Fig. 16, (1 1 0) glide planes were observed, which are oriented nearly orthogonal to the crack front. There is no difference in the shape and glide behaviour of the dislocations, except that the non-screw segments are able to escape to the surface. We assume that these half loops nucleate at the crack tip and expand into the crystal, hence the mobility of the dislocation segments strongly depends on their crystallographic orientation.

4. Discussion

The in situ observations of the microprocesses near the crack tip enable us to derive some conclusions regarding the different behaviour between NiAl single crystals loaded in ⟨1 0 0⟩ directions and crystals loaded in non-⟨1 0 0⟩ directions. Based on the detailed knowledge of the dislocation structure and the crack and dislocation dynamics, a semi-quantitative description should be possible in the future.

The tensile straining experiments with 'soft' crystals confirmed that localized plastic deformation near the crack tip plays an important role in crack propagation. The operating Burgers vector of the corresponding dislocations was always of the type ⟨1 0 0⟩. Shear processes favor crack growth as suggested in Ref. [3]. A direct correlation was observed between (i) the emission and the viscous motion of shear loops or half loops on the {1 1 0} cleavage planes and (ii) a smooth crack propagation. These loops on {1 1 0} planes exhibit an angular shape near the screw direction, caused by the elastic instability of dislocation segments with screw character. Before segments of these dislocations are able to cross-slip, it is necessary to force them into the screw orientation. This seems to be relatively easy in very thin foils – here cross–slip is very frequent, as demonstrated in Fig. 4. Then, the dislocations at the crack tip were emitted almost homogeneously into a fan-shaped region ahead of the crack tip. In thicker crystals cross-slip is obstructed. Only when the local stress is strongly increased, avalanche-like cross-slip processes occur. This restriction in cross-slip diminishes the number and

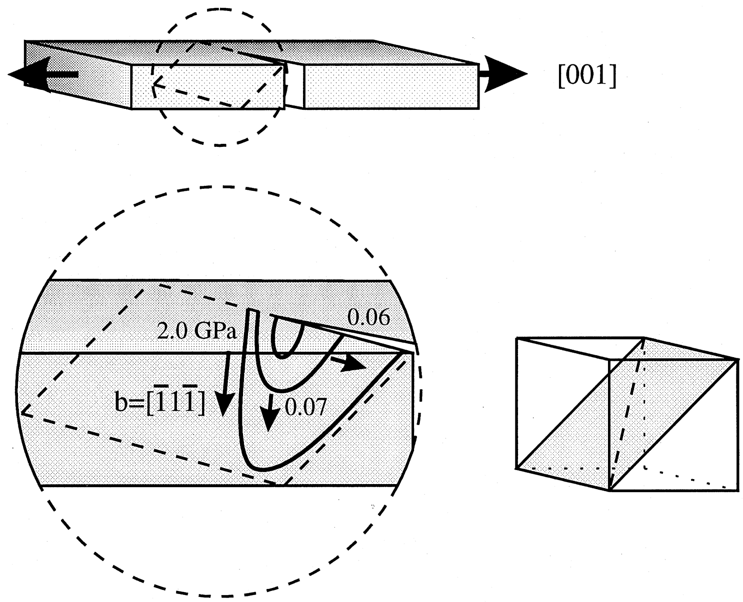

Fig. 16. Schematic drawing of the slip geometry of dislocations shown in Fig. 15.

especially the spreading of dislocation sources, which are required to enable plastic deformation and to relax local stresses.

During straining in [1 $\bar{1}$ 0] direction the preferred cleavage planes are the inclined {1 1 0} planes. The (1 1 0) plane, which lies in edge-on orientation is not activated, confirming that dislocation glide processes on planes parallel to the respective cleavage planes favor crack growth. For tensile straining along [1 $\bar{1}$ 0], the [0 0 1](1 1 0) slip system is not activated by macroscopic stress. On the microscopic scale the cleavage planes mostly deviate from the ideal {1 1 0} planes. While penetrating the plastic zone, the crack typically exhibits no faceting; it does not jump between different {1 1 0} planes or well-defined high-index planes (as e.g. in Ref. [4]). Instead, the crack is smoothly curved. Changing the strain rate influences this process. Higher strain rates result in coarser deviations from the {1 1 0} plane, i.e. the crack structure becomes more faceted.

On changing the tensile direction towards [1 $\bar{1}$ 1], additional slip systems are activated. Dislocation interactions become more frequent, the lack of dislocation sources is compensated for, and plastic deformation occurs in a larger region. Thus, the propagation of the crack is hindered, its structure is less regular; therefore the local stress should be reduced, and the fracture toughness increased.

Straining in the 'hard' crystal orientations revealed that on a microscopic level the crack propagation always involves plastic deformation, too. Compared to the 'soft' orientation, however, the plastic zone remains much smaller. Plastic deformation is restricted to a zone at the crack tip being a few micrometer wide and to extremely localized dislocation slip bands.

The slip system activated by the macroscopic stress is of the type $\langle 1\,1\,1\rangle\{1\,1\,0\}$. Dislocation segments of edge or mixed character are relatively mobile. Theoretical values of the Peierls stress are in the same order of magnitude as for dislocations on the primary $\langle 1\,0\,0\rangle\{1\,0\,0\}$ slip system [9]. Accordingly, such dislocation segments form within a narrow slab, which is less than 0.5 μm wide, with a high density parallel to the crack face. If those dislocations penetrate deeper into the crystal, starting as half loops at the crack tip, some segments rotate into screw orientation. Their Peierls stress is about two orders of magnitude higher than that of the edge type segments, so that they are nearly immobile. As a consequence, they shield the successive dislocations and inhibit their motion. Moreover, owing to the negligible cross-slip probability, a lack of dislocation sources arises. Both effects inhibit plastic deformation in a larger region.

Local stress concentrations and/or a rotation of the tensile axis are responsible for the activation of the extended slip bands at further straining. When straining along [0 0 1], slip in $\langle 1\,0\,0\rangle$ directions is not activated by the macroscopic stress. Owing to the localized nature of these slip bands mentioned above, the relaxation of the stress is very limited at a macroscopic scale. In front of the crack tip, the bands are relatively strong obstacles to the propagation of the crack. Especially in samples with (1 1 0) surfaces, a strong deviation of the crack from its former direction is often observed at these slip bands. On the other hand, the bands are also obstacles for dislocation motion. Dislocations hardly propagate into the region beyond the bands, as long as the crack stops at this position. Thus, an extended plastic zone does not develop.

5. Conclusions

On the microscopic scale, crack propagation in NiAl always involves plastic deformation, even if strained at room temperature in 'hard' directions. For 'soft' directions, dislocation emission at the crack tip and crack growth are directly correlated. However, with increasing dislocation density the crack gets shielded. These competing processes control crack growth, often resulting in a discontinuous propagation. During straining in a 'hard' direction, dislocations on the $\langle 1\,1\,1\rangle\{1\,1\,0\}$ slip system are activated near the crack tip, but their mobility is strongly restricted where they rotate into the screw orientation. Thus, cross slip and the creation of dislocation sources are also inhibited. Both, the immobility of these dislocations and the lack of dislocation sources are reasons for the RT brittleness.

Acknowledgements

The authors would like to thank U. Essmann and R. Henes from the Max-Planck-Institut für Metallforschung for providing the NiAl single crystal. We acknowledge the staff of the HVEM facility in Halle for their continuous help, and we are grateful for the financial support by the Deutsche Forschungsgemeinschaft.

References

[1] Darolia R, Lahrman DF, Field RD, Dobbs JR, Chang KM, Goldman EH, Konitzer DG. In: Liu CT et al., editors. Ordered intermetallics – Physical metallurgy and mechanical behaviour. Dordrecht: Kluwer Academic Publishers, 1972:679–98.
[2] Miracle DB. Acta Metall Mater 1993;41:649–84.
[3] Yoo MH, Sass SL, Fu CL, Mills MJ, Dimiduk DM, George EP. Acta Metall Mater 1993;41:987–1002.
[4] Darolia R. JOM 1991;43:44.
[5] Vehoff H. In: Liu CT et al., editors. Ordered intermetallics – Physical metallurgy and mechanical behaviour. Dordrecht: Kluwer Academic Publishers, 1972:299–320.
[6] Messerschmidt U, Appel F. Ultramicroscopy 1976;1:223.
[7] Messerschmidt U. In: Rotbarts, Wilson AJ, editors. Procedures in electron microscopy, ch. 9.12. Wiley, Chichester, 1993.
[8] Messerschmidt U, Haushälter R, Bartsch M. Mater Sci Eng A 1997;234–236:822.
[9] Schroll R, Gumbsch P, Vitek V. Mater Sci Eng A 1997;233:116–20.